

Prolactin Mediates Long-Term, Seasonal Rheostatic Regulation of Body Mass in Female Mammals

Christopher J. Marshall,¹ Alexandra Blake,² Calum Stewart,³ T. Adam Liddle,³ Irem Denizli,³ Fallon Cuthill,³ Neil P. Evans,³ and Tyler J. Stevenson³ 

¹School of Physiology, Pharmacology and Neuroscience, University of Bristol, Bristol BS8 1TD, UK

²Institute of Molecular Biology, University of Mainz, Mainz 55122, Germany

³School of Biodiversity, One Health and Veterinary Medicine, University of Glasgow, Glasgow G61 1QH, UK

Correspondence: Tyler Stevenson, PhD, School of Biodiversity, One Health and Veterinary Medicine, University of Glasgow, Switchback Rd, Garscube Campus, Glasgow G61 1QH, UK. Email: tyler.stevenson@glasgow.ac.uk

Abstract

A series of well-described anabolic and catabolic neuropeptides are known to provide short-term, homeostatic control of energy balance. The mechanisms that govern long-term, rheostatic control of regulated changes in energy balance are less well characterized. Using the robust and repeatable seasonal changes in body mass observed in Siberian hamsters, this report examined the role of prolactin in providing long-term rheostatic control of body mass and photoinduced changes in organ mass (ie, kidney, brown adipose tissue, uterine, and spleen). Endogenous circannual interval timing was observed after 4 months in a short photoperiod, indicated by a significant increase in body mass and prolactin mRNA expression in the pituitary gland. There was an inverse relationship between body mass and the expression of somatostatin (*Sst*) and cocaine- and amphetamine-regulated transcript (*Cart*). Pharmacological inhibition of prolactin release (via bromocriptine injection), reduced body mass of animals maintained in long photoperiods to winter–short photoperiod levels and was associated with a significant increase in hypothalamic *Cart* expression. Administration of ovine prolactin significantly increased body mass 24 hours after a single injection and the effect persisted after 3 consecutive daily injections. The data indicate that prolactin has pleiotropic effects on homeostatic sensors of energy balance (ie, *Cart*) and physiological effectors (ie, kidney, BAT). We propose that prolactin release from the pituitary gland acts as an output signal of the hypothalamic rheostat controller to regulate adaptive changes in body mass.

Key Words: homeostasis, cocaine- and amphetamine-regulated transcript, adipose tissue, bromocriptine, somatostatin

Abbreviations: *Agrp*, agouti-related peptide; BAT, brown adipose tissue; Bromo, bromocriptine; *Cart*, cocaine- and amphetamine-regulated transcript; LD, long day; *Npy*, neuropeptide Y; PH, posterior hypothalamus; Prl, prolactin; Prlr, prolactin receptor; qPCR, quantitative polymerase chain reaction; SD, short day; *Sst*, somatostatin; Th, tyrosine hydroxylase; Vgf, VGF nerve growth factor inducible.

Homeostasis is a fundamental concept used to describe how endocrine systems maintain stability despite significant environmental change (1). The principles of control theory were used to define how a physiological variable is regulated, around a specific set point, using sensors, error detection, controllers, and effectors (2). However, homeostasis is limited to the explanation of short-term responses to external and internal physiological perturbations. Long-term daily and seasonal changes in physiological set points, sensory detection systems, controllers, and effector function do not adhere to homeostatic principles (3); also see (4) for an exhaustive list). The concept of rheostasis, or programmed, regulated changes in set points was therefore proposed to account for long-term oscillations in physiological systems (4). Since the genetic revolution of the 1990s, massive gains in our understanding of the genetic, cellular, and systems control of homeostasis (including energy regulation) have been achieved. However, less is known about the “controller” mechanisms that govern programmed rheostatic regulation of energy balance.

With regard to the short-term homeostatic regulation of energy balance in mammals, a series of neuroendocrine peptides

in the arcuate nucleus such as neuropeptide Y (*Npy*) and agouti-related peptide (*Agrp*), are key targets of autonomic and endocrine feedback signals from peripheral tissues (eg, adipose tissue) (5, 6). These neuropeptides are highly sensitive to acute challenges in energy balance associated with meal timing or food restriction and trigger compensatory changes, often mediated by changes in circulating leptin (7). In contrast, these orexigenic neuropeptides are not involved in the regulation of the long-term oscillations in food intake and body mass that occur across seasons (8).

The Siberian hamster (*Phodopus sungorus*) is an excellent animal model to examine these programmed rheostatic changes in energy balance due to its robust, reliable, and repeatable seasonal oscillations in body mass (9, 10). In laboratory conditions, under a long summer photoperiod (eg, light for 16 hours, darkness for 8 hours), hamsters maintain a large body mass and high daily food intake. A simple shift to a short winter photoperiod (eg, 8 light:16 dark), will induce a 30% to 40% reduction in body mass (11–14), decreased daily food intake (12) and loss of intra-abdominal adipose tissue (15). However, prolonged exposure to short photoperiod results

in the spontaneous reversion back to heavier body mass and increased food intake observed in the long photoperiod physiological condition (14). This long-term programmed change in energy metabolism is controlled by an endogenous circannual timer that is approximately 6 months in length and serves to anticipate spring environmental conditions (16). The photoperiod-induced change in body mass provides a powerful model to examine the regulated changes in physiological set points of programmed energy rheostasis.

In hamsters, anorexigenic neuropeptides neuropeptide *y* (*Npy*) and agouti-related peptide (*Agrp*) and circulating hormones (ie, leptin) remain sensitive to short-term, homeostatic challenges, such as food restriction, and increase transcript expression in both long- and short-photoperiod conditions (14, 17, 18). Multiple studies have established that many of the neuropeptides associated with food intake and energy homeostasis, including *Npy* and *Agrp*, are constitutively expressed across photoinduced seasonal energy states (14, 16). Under short photoperiod conditions, hamsters become leptin-resistant and hypophagic compared with hamsters maintained in long photoperiod (19). It is known that several neuropeptides that control growth, such as somatostatin (*Sst*; also abbreviated *Srif*) (20), cocaine- and amphetamine-regulated transcript (*Cart*) (21) and VGF nerve growth factor inducible (*Vgf*) (22, 23) are regulated by photoperiod. Pro-opiomelanocortin (*Pomc*) has also been implicated in the control of seasonal energy balance (8). Studies taking advantage of pasireotide, a potent somatostatin agonist, established that pharmaceutical reduction in the growth hormone axis activity mimicked short-photoperiod-induced changes in body mass (24-26). *Sst* is a prime candidate for regulation of photoperiod-induced changes in energy metabolism due to strong inhibitory effects on both growth hormone and prolactin release from the pituitary gland (27).

Prolactin is an evolutionarily conserved hormone produced in the pituitary gland that impacts a multitude of neuroendocrine systems (28, 29). Of relevance, prolactin regulates longer-term changes in energy homeostasis during pregnancy and lactation (30). In hamsters, prolactin mRNA changes according to the photoinduced seasonal state, with a positive relationship between transcript expression in the pars distalis and body mass (14). Previous studies have shown prolactin can prevent short-photoperiod-induced changes in pelage color (31) and reduced body mass (32) in Siberian hamsters. Conversely, daily administration of bromoergocryptine, a potent inhibitor of prolactin release, can maintain the long photoperiod pelage (31). Despite clear links between prolactin and photoinduced changes in peripheral physiology, the evidence for any change in the neuroendocrine control mechanisms, such as orexigenic or anorexigenic neuropeptides is uncharacterized. In sheep, the secretion of prolactin oscillates with a period that nearly matches an annual cycle, with a peak in spring and a nadir in autumn or winter, and the lactotrophs are proposed to provide an endogenous circannual timing mechanism (33). We have recently established using transcriptomic profiling in Siberian hamsters, that the prolactin mRNA receptor is widely expressed in peripheral tissues such as the uterus, kidneys, and adipose tissue (34). Given that changes in prolactin mRNA expression coincide with changes in hamster body mass, and prolactin receptors are expressed in a range of peripheral tissues (eg, adipose), it could be hypothesized that prolactin may function as an output of the neuroendocrine controller necessary for programmed rheostatic changes in seasonal body mass.

To test this hypothesis 3 studies were conducted. The first study investigated the impact of photoperiod-induced decrease in body mass and the subsequent endogenous circannual interval timer induced growth in hamster body mass. By taking a high-sampling resolution during onset and progression of the circannual interval provided a unique opportunity to identify programmed changes in key neuroendocrine peptides such as *Sst*, and *Cart* expression. Neuropeptide expression could then be examined to map out the relationship with long-term regulated programmed changes in prolactin mRNA expression. The second study used the dopamine receptor agonist bromocriptine to investigate the impact of reduced prolactin on hamster body mass and neuroendocrine peptides associated with long-term control of energy balance. The third study investigated the acute effects of ovine prolactin on hypothalamic *Sst* and *Cart* expression and its ability to induce growth of peripheral tissues and increase body mass. The findings illustrate that prolactin has robust and repeatable effects on long-term changes in hamster body mass and has pleiotropic effects in the hypothalamus and on several peripheral tissues.

Materials and Methods

Ethical Permission

All procedures were approved by the University of Glasgow Animal Welfare and Ethics Review Board and conducted under the UK Home Office Project License.

Animals

Female Siberian hamsters (*Phodopus sungorus*) were housed in the Veterinary Research Facility, University of Glasgow on a long-day (LD) photoperiod (16 light:8 dark) and humidity at 55%. Hamsters were group housed with ad libitum access to rodent chow (Harlan Tekland) and water.

Study 1: Circannual Interval Timing

N = 53 female hamsters were used to examine the endogenous and long-term control of energy balance (Fig. 1A). A subset of juvenile hamsters (2 months of age [2 m]; n = 4) was selected as a pre-photoperiod manipulation reference group. Then hamsters were divided into 2 photoperiod treatment groups: (i) animals held on long-day photoperiod (n = 13) that served as a reference group; or (ii) animals transferred to short-day (SD) photoperiod (n = 36) (8 light:16 dark) to allow the investigation of the endogenous change in energy balance driven by the circannual interval timer (35). The long-day photoperiod reference groups were killed, and tissues collected at either 3 months (LD3; n = 7) or 10 (LD10; n = 6) months of age. To obtain high-resolution data from the circannual interval timer sampling group, hamsters transferred to SD were euthanized and tissues were collected at 3 (SD3; n = 7), 4 (SD4; n = 4), 5 (SD5; n = 9), 6 (SD6; n = 9), and 7 (SD7; n = 7) months of age. Prior to euthanasia, pelage color and body mass were measured. Animals were euthanized by cervical dislocation followed by rapid decapitation during the early light phase (3-5 hours after light onset) and the brain and pituitary gland tissues were dissected and immediately frozen on dry ice. Tissues were stored at -70 °C until RNA extraction. The experiment used archived tissue samples for LD2 and LD3, but unfortunately, molecular analyses of the pituitary gland could not be conducted in these animals. Archival tissue provides a

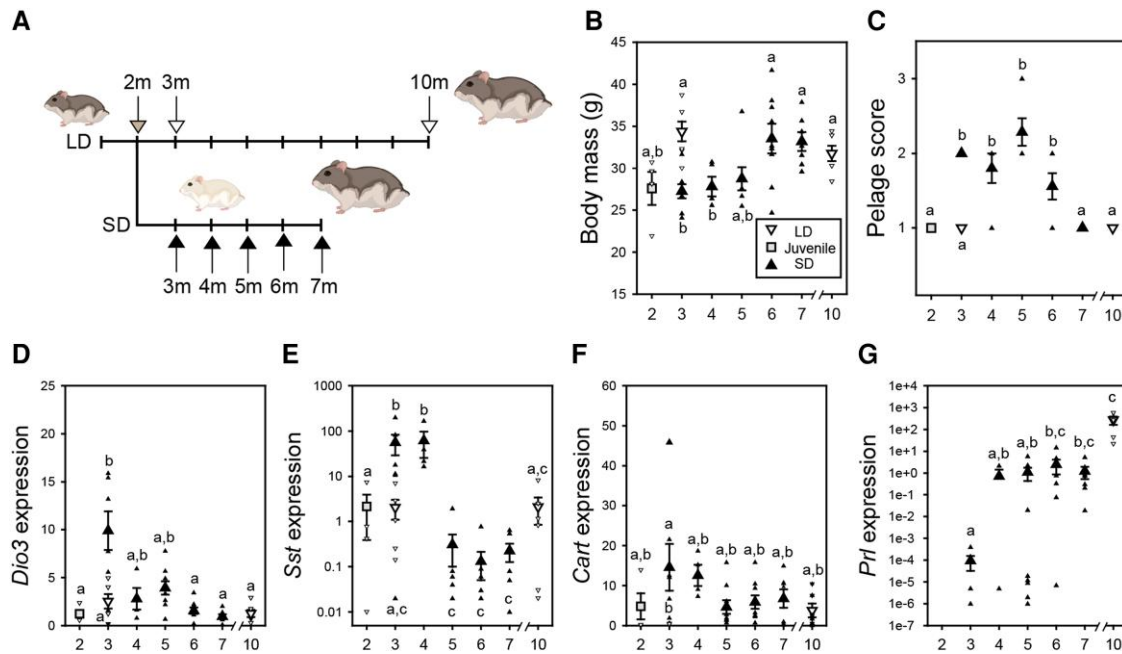


Figure 1. Circannual interval timer programs changes in hamster energy balance. (A) Schematic representation of the experimental design. (B) hamsters kept in the long photoperiod (LD) condition maintained heavy body mass from 2 months of age (ie, juvenile) to 10 months of age (ie, adult). Hamsters transferred to short photoperiod (SD) had lower body mass until 5 months of age (5 m). The endogenous circannual timing of growth is reflected by the gradual increase in body mass in short photoperiod hamsters from 4 months (4 m) of age to 6 months of age (6 m). (C) Hamster maintained in LD have a dark agouti pelage (score 1), transfer to SD induced a white pelage color (score 3) which reverts to the agouti color. (D) Hypothalamic expression of deiodinase type 3 (*Dio3*) is significantly increased in hamsters exposed to SD (ie, 3 m) which then is reduced to LD levels. (E) Somatostatin (*Sst*) expression was significantly increased after transfer to SD and then after 2 months there was a significant inhibition which returned to LD levels. (F) Cocaine- and amphetamine-regulated transcript (*Car1*) displayed a transient increase in expression when exposed to SD, which was subsequently decreased to LD levels. (G) Prolactin (*Prl*) gradually increased in hamsters' exposure to SD. Hamsters in LD had significantly greater *Prl* expression compared with all SD groups. X-axis is the age of hamster for all panels. Letters denote significant differences between treatment groups. The gray box denotes LD housed juvenile hamsters, downward white triangles indicate LD, and upward black triangles indicate SD light conditions. Residual plots indicate individual data points. All data are mean \pm SEM.

valuable approach to reduce the need for extra animals and directly addresses the mission of the National Centre for the Replacement, Reduction, and Refinement of animals in research.

Study 2: Necessity of Prolactin for Long-Term Control of Energy Balance

A total of $N = 23$ female hamsters were used to examine the effects of pharmaceutically reduced prolactin on photoperiod-induced changes in body mass, neuroendocrine and pituitary gland transcripts, and tissue mass (Fig. 2A). Adult (3-8 months of age) females were raised in a long-day photoperiod. Hamsters were pseudorandomly assigned by body mass to either long ($n = 15$) or short ($n = 8$) day photoperiod treatments for 4 weeks. Long-day photoperiod hamsters were further divided into 2 groups. The first group ($n = 8$) served as the long-day photoperiod reference group and received subcutaneous injections of saline for 4 weeks. The second group ($n = 7$) received daily injections (12 $\mu\text{g/g}$ body mass) of the dopamine receptor agonist bromocriptine (Bromo) (Sigma-Aldrich; cat# B2134) in saline to reduce circulating prolactin. This dose was selected based on previous work using Bromo in Siberian hamsters (32). The short-day photoperiod control treatment hamsters received daily subcutaneous injections of saline for the duration of the study. All injections started when hamsters were moved to short-day photoperiod and occurred during the light phase (7-8 hours after lights on). Body mass and daily food intake were

measured before photoperiod treatment (Pre) and then at 1, 2, 3, and 4 weeks of treatment. Body mass and food weight were collected at the midpoint of the light phase. At 4 weeks, hamsters were humanely euthanized by cervical dislocation followed by rapid decapitation 3 to 5 hours after light onset, and brain and pituitary tissues harvested and stored, consistent with Study 1. Brown adipose tissue (BAT), kidney, uterine, and splenic tissues were also dissected, weighed to the nearest milligram, frozen on dry ice and stored at -70°C until RNA extraction.

Study 3: Sufficiency of Prolactin for Short-Term Control of Energy Balance

The impact of prolactin on the short-term neuroendocrine control of photoperiod-induced changes in body mass was investigated with $N = 25$ hamsters (Fig. 3A). Adult (3-8 months of age) females raised in the long-day photoperiod were transferred to short-day photoperiod for 8 weeks to induce body mass loss and low circulating prolactin concentrations. Hamsters were then pseudorandomly assigned by body mass to daily intraperitoneal injections of either 100 μL vehicle control (50% dimethyl sulfoxide + 50% saline) ($n = 12$) or 18 μg prolactin (NIAMDD-O-PRL) dissolved in vehicle ($n = 13$). This dose was similar to those used in previous research, demonstrating that established long-term prolactin administration could induce agouti hair pelage in short-day photoperiod Siberian hamsters (32, 36). Hamsters were injected (vehicle or prolactin) during the middle of the light phase and either

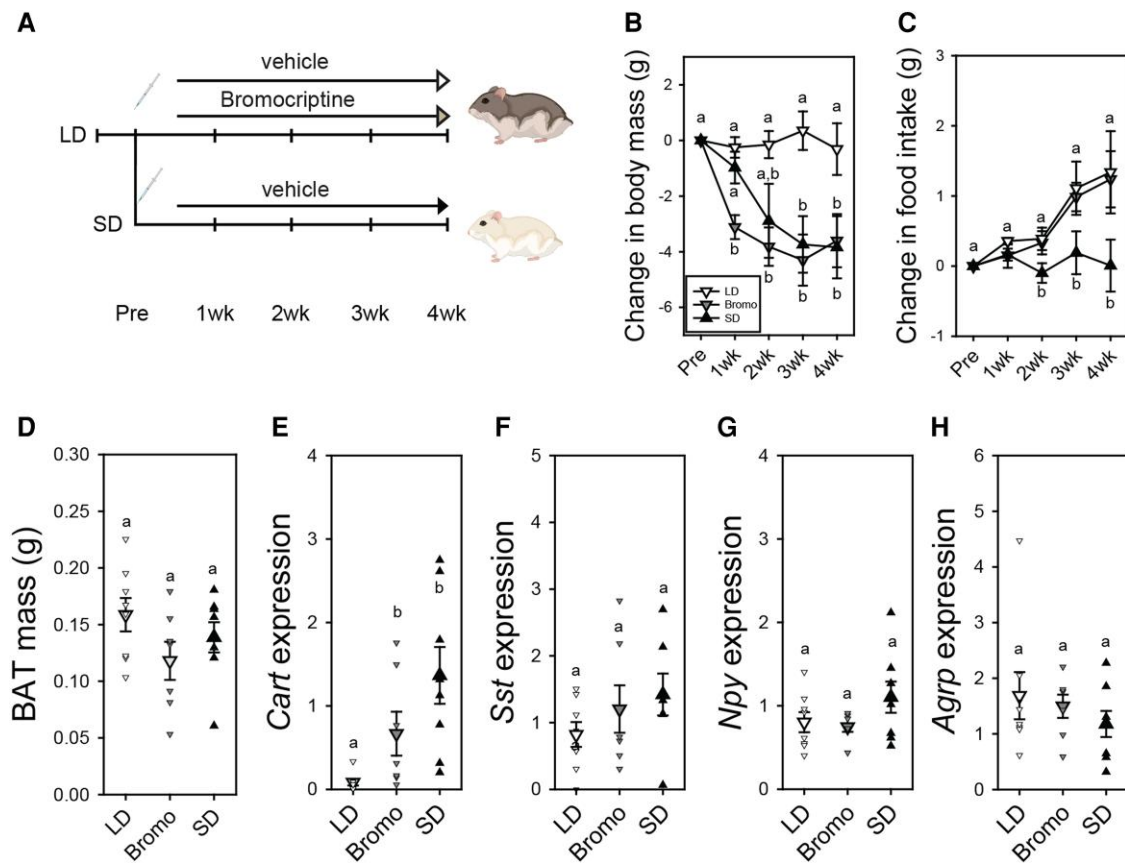


Figure 2. Necessity of prolactin to drive long-term changes in hamster body mass. (A) Schematic representation of the experimental design. (B) Short photoperiod (SD) and bromocriptine (Bromo) treatment significantly reduced hamster body mass. (C) Hamsters housed in SD ate significantly less food over a 24-hour sampling period compared with both long photoperiod (LD) controls and Bromo-treated groups. (D) BAT mass (E) Somatostatin (*Sst*) (F) Cocaine- and amphetamine-regulated transcript (*Cart*) expression was significantly elevated in SD hamsters. There was no significant effect of photoperiod or Bromo treatment on neuropeptide Y (*Npy*) (G) or agouti-related peptide (*Agrp*) (H). Letters denote significant differences between treatment groups. Downward white triangles indicate LD, downward gray triangles indicate Bromo treatment, and upward dark triangles indicate SD condition. Residual plots indicate individual data points. All data are mean \pm SEM.

injected and killed 24 hours later (1d; 6–7 hours after light onset) or received injections on 3 consecutive days (3d). The injection schedule was oriented so that all hamsters were euthanized on the same calendar day. On the last day, body mass was measured, and animals were humanely killed by cervical dislocation followed by rapid decapitation. Kidneys, BAT, uteri, and spleens were weighed on to the nearest milligram, frozen on dry ice and stored at -70°C .

Tissue Preparation, RNA Extraction, and cDNA Synthesis

Prior to hypothalamic tissue dissection, the brain was placed in a Leica CM1850 cryostat chamber (Leica Biosystems, Germany) and warmed to -20°C for 30 minutes. Each brain was placed within a steel coronal mouse brain matrix (1.0-mm thickness) with the ventral surface of the brain exposed. Brain slices were collected between -0.34 mm and -2.46 mm to isolate tissue containing the posterior hypothalamus (PH). The PH was then separated from other brain structures by a transverse cut aligning the dorsal aspect of the optic tracts. This tissue dissection of the PH is specific to the arcuate nucleus and cells surrounding the third ventricle as evidenced by molecular localization demonstrated in our previous publication (37). All samples were returned to -70°C until RNA extraction.

Tissue was homogenized in TRIzol reagent (ThermoFisher Scientific), and RNA was extracted according to manufacturer instructions. Genomic DNA and trace organic contaminants were removed from each sample using RNase-free DNase (Qiagen), followed by purification using RNeasy MinElute Cleanup kit (Qiagen). RNA concentrations were measured via NanoDrop (A260/280 ratio). cDNA was synthesized using a Precision nanoScript 2 Reverse Transcription kit (PrimerDesign). RNA concentration was normalized across samples to either 1 μg (PH samples) or 200 ng (pituitary samples) up to a total of 9 μL in RNase-free water and 1 μL of oligo dT primer added. The cDNA synthesis was performed per manufacturer instructions, and samples were brought to a total volume of 100 μL and stored at -20°C .

Quantitative Polymerase Chain Reaction

Quantitative polymerase chain reaction (qPCR) was performed on cDNA samples to measure the relative expression of transcripts of interest. Samples were run using a 96-well plate, with each reaction consisting of 4.8 μL of Brilliant II SYBR green qPCR master mix (Agilent) with forward and reverse primers of the transcripts of interest (24:1 ratio) and 4.8 μL of cDNA. To examine molecular substrates that underlie programmed rheostatic control of energy balance, primer

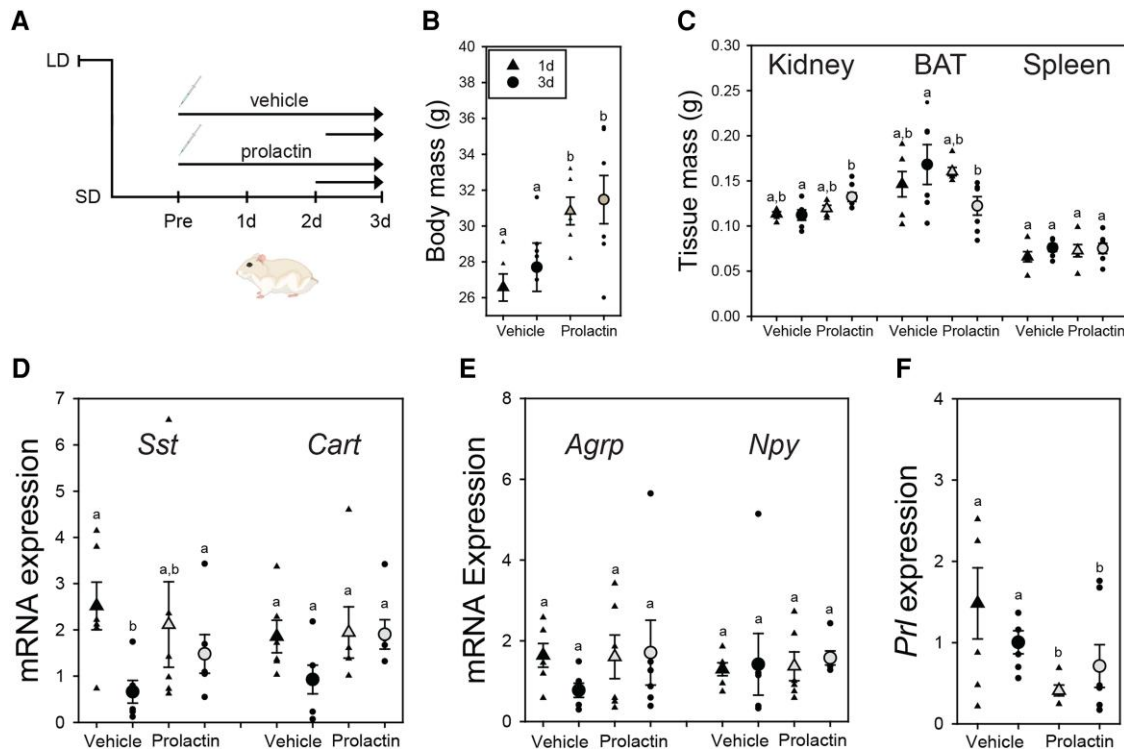


Figure 3. Prolactin is sufficient to increase hamster body mass. (A) Schematic representation of the experimental design. (B) Prolactin was sufficient to increase body mass 24 hours after a single injection, and after 3 consecutive daily injections. (C) Prolactin significantly increased kidney mass after 3 days, reduced BAT mass after 3 days and had no effect on spleen mass. (D) Somatostatin (*Sst*) was higher in hamsters injected with prolactin for 3 days compared with vehicle-treated animals. (E) There was no significant effect of prolactin on agouti-related peptide (*Agrp*) or neuropeptide Y (*Npy*) expression. Prolactin injections were sufficient to inhibit pituitary gland pituitary mRNA (*Prl*) expression compared with vehicle controls. Letters denote significant differences between treatment groups. Upward triangles indicate animals injected once (1d) and circles indicate animals injected for 3 days (3d). Black filled objects denote short photoperiod vehicle control groups and gray filled objects indicate prolactin-treated hamsters. Residual plots indicate individual data points. All data are mean \pm SEM.

pairs were used that targeted *Sst*, *Cart*, *Npy*, *Agrp*, *Dio3*, *Th*, *Tsh β* , *Prl*, *Prlr*, and *Gh* (Supplementary Table S1 (38)). Reference transcripts that were selected based on a previous publication (39) that demonstrated high stability included *18 seconds*, *Gapdh* and *Hprt* (Supplementary Table S1 (38)). Reactions were carried out in duplicate and run with non-template negative controls in an Mx3000P qPCR system (Agilent) using the following thermal cycling conditions: (i) initial denaturation at 95 °C for 7.5 minutes followed by 40–45 cycles of (ii) denaturation at 95 °C for 30 seconds, (iii) annealing at temperature specified for each respective gene in Supplementary Table S1 (38) for 30 seconds, and (iv) extension at 72 °C for 30 seconds. Melt curves were generated for each sample to confirm the specificity of each reaction. Reaction efficiency and cycle threshold were assessed in PCR Miner (40). The relative mRNA expression of each gene was determined in relation to the mean Ct and normalized to the reference gene with the best stability and then calculated as fold difference from the control group using the formula $2^{-\Delta\Delta Ct}$.

Statistical Analyses

Raw data are provided in Supplementary Table S2 (38). One-way ANOVAs were used to examine statistical significance of all dependent variables for Study 1. In Study 2, a 2-way repeated ANOVA (factors: week and treatment) was conducted on body mass and food intake. One-way ANOVAs were conducted to examine the effect of treatment on tissue mass, and hypothalamic and pituitary transcript expression. For Study 3,

a 2-way ANOVA was conducted on body mass, tissue mass, and transcript expression levels. Kolmogorov-Smirnov tests were conducted to confirm normality; when violation of normality was identified, the data were log-transformed before statistical analyses. Statistical significance was determined as $P < .05$. Data are presented as mean \pm standard error of the mean.

Results

Study 1: Circannual Interval Timing of Body Mass Involves Programmed Changes in Neuropeptides

As anticipated, there was a significant effect of photoperiod on female body mass ($F_{7,45} = 4.89$; $P < .001$). Body mass in female hamsters transferred to short-day photoperiods did not change from 3 (SD3) to 4 (SD4) months of age (Fig. 1B). Body mass of short-day-photoperiod housed females was significantly increased by 6 (SD6) months of age ($P < .05$). There were no significant differences between hamsters housed in short day photoperiod for either 6 or 7 (SD7) months and they did not differ compared with long-day photoperiod control adults (LD10) ($P > .96$). Pelage color changed significantly with the onset of the circannual interval timer ($F_{7,45} = 22.29$; $P < .001$) (Fig. 1C). All hamsters in long-day photoperiod maintained the dark agouti pelage color (ie, rated 1) throughout. Exposure to short-day photoperiod (SD3, SD4, SD5, and SD6) increased ($P < .05$) the pelage color rank, indicative of a white fur coat. All SD7 hamsters had returned to pelage color seen in the LD10 reference group.

Hypothalamic *Dio3* expression varied significantly with photoperiod ($F_{7,45} = 4.58$; $P < .001$) (Fig. 1D). Hamsters in SD3 had a significant ($P < .05$) but transient increase in hypothalamic *Dio3* expression, and thereafter levels were comparable to LD10 controls. Pars tuberalis *Tshb* expression varied significantly across photoperiod treatment groups ($F_{7,40} = 3.62$; $P < .005$) (Supplementary Fig. S1A (38)). LD10 controls had significantly higher *Tshb* expression compared with SD5 hamsters. There was a trend for significantly higher levels of *Tshb* in LD10 compared with SD4 ($P = .05$).

To explore potential changes in neuropeptides involved in long-term programmed changes in energy balance and prolactin secretion, we examined the expression profile of hypothalamic *Sst*, *Cart*, and *Th*, respectively. We identified that hypothalamic *Sst* expression was significantly affected by photoperiodic condition ($F_{7,45} = 7.82$; $P < .001$) (Fig. 1E). *Sst* expression was significantly higher in hamsters housed in short photoperiod during SD3 and SD4 ($P < .05$) before declining to long photoperiod levels. There was no significant difference between LD3 and LD10 photoperiod groups. Hypothalamic tyrosine hydroxylase (*Th*) expression exhibited similar significant changes in expression when animals were transferred to short photoperiod ($F_{7,45} = 9.41$; $P < .001$) (Supplementary Fig. S1B (38)). *Th* expression was higher ($P < .05$) in SD3 and SD4 compared with LD3 and LD4 hamsters. Hypothalamic *Cart* expression varied significantly across the photoperiod treatment groups ($F_{7,45} = 2.45$; $P < .05$) (Fig. 1F). Transfer to a short photoperiod induced a significant ($P < .05$) increase in *Cart* expression in SD3 compared with LD3 hamsters. These data demonstrate a rapid and significant increase in multiple transcripts associated with the inhibition of growth (ie, *Sst*, *Cart*) and prolactin release (ie, *Th*) during early exposure to short photoperiods and then subsequently a decline in expression during the progression of the endogenously increases in body mass.

Next, we examined expression levels of *Prl* and *Gh* mRNA in the pituitary gland. Pituitary *Prl* expression changed significantly during short photoperiod exposure ($F_{5,33} = 9.22$; $P < .001$) (Fig. 1G). There was a rise in *Prl* levels from SD3 to SD4 ($P < .05$). SD3, SD4 and SD5 were significantly lower compared with LD10 ($P < .05$). There was a significant difference in *Gh* expression across the treatment groups ($F_{5,33} = 4.8$; $P < .005$) (Supplementary Fig. S1C (38)). LD10 hamsters had significantly higher *Gh* expression compared with all SD animals ($P < .001$). There was no significant difference in *Gh* expression between the short photoperiod treatment groups ($P > .88$).

Study 2: Bromocriptine Induced Body Mass Reductions and Hypothalamic Neuropeptide Expression

There was a significant interaction between effect of treatment and time on body mass ($F_{8,80} = 4.18$; $P < .001$) (Fig. 2B). One week after treatment, the Bromo-injected long-day (Bromo) hamsters had significantly ($P = .01$) lower body mass compared with control LD hamsters, and a trend ($P = .05$) was noted for a lower body mass in Bromo compared with SD hamsters. There was no significant difference between SD and LD ($P = .49$). After 2 weeks, LD hamsters were significantly heavier compared with the Bromo ($P < .001$) and SD ($P < .05$) hamsters, with no significant difference between Bromo and SD animals ($P = .39$). At 3 weeks and 4 weeks, the pattern continued, with Bromo and SD hamsters both

having significantly reduced body mass compared with LD hamsters ($P < .005$). There was no significant difference between Bromo and SD hamsters ($P > .61$). There was a significant treatment by week interaction for food intake ($F_{8,72} = 2.36$; $P < .05$) (Fig. 2C). There was no significant difference between any treatment group during 1 week ($P = .61$). During 3 to 4 weeks, SD hamsters ate significantly ($P < .05$) less food compared with LD and Bromo-injected hamsters. There was no difference ($P = .76$) between LD and Bromo-injected hamsters at any time point studied. These data establish that long-term changes in body mass but not food intake are impacted by Bromo treatment in hamsters.

Neither BAT mass ($F_{2,20} = 1.82$; $P = .18$) (Fig. 2D), uterine mass ($F_{2,20} = 2.21$; $P = .13$) (Supplementary Fig. S2A (38)), kidney mass ($F_{2,20} = 0.03$; $P = .97$) (Supplementary Fig. S2B (38)), or spleen mass ($F_{2,20} = 0.06$; $P = .94$) (Supplementary Fig. S2C (38)) were affected by photoperiod or treatment.

To determine if the long-term changes in body mass were impacted by hypothalamic neuropeptides, we measured *Cart* and *Sst* expression. There was a significant effect of treatment on hypothalamic *Cart* expression ($F_{2,19} = 11.1$; $P < .001$) (Fig. 2E). *Cart* expression was significantly lower in LD compared with Bromo ($P < .05$) and SD ($P < .001$) hamsters. There was no significant difference between Bromo and SD hamsters ($P = .27$). There were no effects of photoperiod or treatment on *Sst* ($F_{2,19} = 1.16$; $P = .33$) (Fig. 2F). These data establish that *Cart* expression is significantly impacted by long-term treatment with Bromo and suggests that prolactin may provide inhibitory input to at least one neuropeptide involved in energy balance. To determine whether neuropeptides associated with food intake and appetite were impacted by Bromo treatment, we measured hypothalamic *Npy* and *Agrp* expression. There was no significant effect on *Npy* ($F_{2,20} = 1.94$; $P = .16$) (Fig. 2G) or *Agrp* ($F_{2,20} = 0.71$; $P = .51$) (Fig. 2H).

To establish the predicted effect of Bromo on circulating prolactin levels, we measured pituitary prolactin mRNA and hypothalamic *Th* and prolactin receptor (*Prlr*) expression. Hypothalamic *Th* expression was significantly different across the treatment groups ($F_{2,19} = 5.83$; $P < .01$). In long-day photoperiod hamsters, there was significantly lower hypothalamic *Th* expression compared with SD controls ($P < .01$). There was no significant difference between Bromo and LD ($P = .34$) and Bromo vs SD ($P = .17$). However, there was one outlier in the LD reference group with a fold-expression value of 3.48 (> 3 standard deviations). Removal of the single measurement shows a significant one-way ANOVA ($F_{2,18} = 13.56$; $P < .001$) with significantly more *Th* in both Bromo ($P < .05$) and SD ($P < .001$) compared with LD hamsters (Supplementary Fig. S2D (38)).

There was no significant effect of treatment or photoperiod on hypothalamic *Prlr* expression ($F_{2,19} = 1.53$; $P = .24$) (Supplementary Fig. S2E (38)). There was a significant effect on *Prl* expression ($F_{2,19} = 5.35$; $P = .01$) (Supplementary Fig. S2F (38)) which was significantly higher in Bromo treatment compared with SD ($P < .01$). There was no significant difference between LD and Bromo ($P = .77$), but there was a trend for higher *Prl* in LD compared with SD ($P = .06$).

Study 3: Prolactin Is Sufficient to Induce Body Mass Growth in Hamsters

Hamsters injected with prolactin were found to have a significant increase in body mass ($F_{1,21} = 12.7$; $P < .005$), but there

was no significant effect of day ($F_{1,21} = 0.62$; $P = .44$) or interaction ($F_{1,21} = 0.04$; $P = .83$) (Fig. 3B). Injection of prolactin was found to significantly increase kidney mass ($F_{1,21} = 8.71$; $P < .01$), but there was no significant effect of day ($F_{1,21} = 1.65$; $P = .21$) or interaction ($F_{1,21} = 2.42$; $P = .12$) (Fig. 3C). There was a significant interaction between prolactin and day on BAT ($F_{1,21} = 4.52$; $P < .05$) (Fig. 3C). However, prolactin injections did not significantly change BAT mass ($F_{1,21} = 0.89$; $P = .35$) nor was there a significant effect of day ($F_{1,21} = 0.88$; $P = .37$). There was no significant effect of day ($F_{1,21} = 1.21$; $P = .28$), prolactin ($F_{1,21} = 0.26$; $P = .61$), or interaction ($F_{1,21} = 0.44$; $P = .51$) on spleen mass (Fig. 3C). There was no significant effect on uterine mass for prolactin ($F_{1,21} = 0.32$; $P = .57$), day ($F_{1,21} = 1.89$; $P = .18$), or interaction ($F_{1,21} = 0.06$; $P = .79$) (Supplementary Fig. S3A (38)).

Sst expression was found to change depending on the day and whether hamsters received a prolactin injection ($F_{1,20} = 4.85$; $P < .05$) (Fig. 3D). *Sst* expression was significantly ($P < .05$) higher in prolactin-treated hamsters on day 3 compared with saline-treated hamsters ($P < .05$). But this may be due to the significant reduction in *Sst* expression on day 3 compared with day 1 of saline treatment ($P < .001$). There was a significant effect of day ($F_{1,20} = 7.28$; $P < .05$), but no effect of prolactin treatment ($F_{1,20} = 0.90$; $P = .35$). There was no significant effect of day ($F_{1,20} = 2.75$; $P = .11$), treatment ($F_{1,20} = 3.31$; $P = .08$), or interaction ($F_{1,20} = 3.62$; $P = .07$) on *Cart* expression (Fig. 3D). *AgRP* was not significantly different between treatment day ($F_{1,20} = 1.47$; $P = .23$), prolactin ($F_{1,20} = 0.13$; $P = .71$) or interaction ($F_{1,20} = 1.56$; $P = .22$) (Fig. 3E). Similarly, there was no significant day ($F_{1,21} = 0.08$; $P = .77$), prolactin ($F_{1,21} = 1.18$; $P = .28$), or interaction ($F_{1,21} = 1.75$; $P = .20$) on *Npy* expression (Fig. 3E).

To confirm prolactin injections were sufficient to mimic circulating hormonal effects we measured pituitary *Prl* expression as a marker of negative feedback. Prolactin injections significantly reduced *Prl* expression ($F_{1,21} = 14.52$; $P < .001$). There was no effect of day ($F_{1,21} = 0.13$; $P = .71$) or interaction ($F_{1,21} = 0.04$; $P = .83$) (Fig. 3F). These data demonstrate that the prolactin dose, and injections were sufficient to activate short-term homeostatic negative feedback mechanisms in female hamsters.

Discussion

This report has shown that *Prl* expression in the pituitary gland is a molecular marker of circannual interval timing of body mass in the Siberian hamster. Increased *Prl* mRNA preceded the endogenous increase in body mass and reversion of pelage color from the winter white fur to the summer agouti color. Using a pharmacological approach, the studies demonstrated the necessity and sufficiency of prolactin to drive a decrease and increase in body mass, respectively. Prolactin effects on body mass appear independent of any change in appetite as Bromo-treated hamsters did not decrease food intake levels. Bromocriptine treatment facilitated an increase, but there was no effect of prolactin administration on hypothalamic *Cart* expression. While prolactin had no effect on BAT or spleen mass, daily prolactin injections significantly increased kidney mass suggesting a role for osmoregulation. These data indicate a robust effect of prolactin on body mass, but no effect on food intake and only minor effects on tissue mass (ie, BAT, kidney) and therefore, suggest that

prolactin induces small effects across tissues which accumulate into a large-scale change in body mass.

Prolactin secretion from the pituitary gland provides an evolutionary conserved output signal for the neuroendocrine control of seasonal physiology (29). Across seasonally breeding animals there is increased secretion of prolactin during periods of breeding and high energy demands. Prior work in Siberian hamsters indicated long-term treatment with bromocriptine, to decrease prolactin concentrations, induced the winter white pelage in long-day housed hamsters (31). Conversely, prolactin injection inhibited the development of the winter white pelage in hamsters housed in short-day photoperiod (31, 36). The results of this study demonstrate that 4 weeks of bromocriptine administration reduced body mass to short photoperiod levels, consistent with previous reports in Siberian hamsters (32). Furthermore, daily administration of prolactin increased body mass which supports previous studies in which loss of body mass in hypophysectomized hamsters was restored to long photoperiod levels with exogenous prolactin administration (41). The data presented here demonstrate that increased circulating prolactin concentrations act to facilitate seasonally programmed changes in body mass.

As an endocrine factor, prolactin can be a powerful output signal to multiple physiological “effector” tissues. Prolactin receptors are distributed widely across many tissues, including those essential for reproduction (ie, uterine, ovary, and testes), osmoregulation (ie, kidney), and energy balance (eg, adipose, liver) (39). Prolactin receptors belong to the cytokine receptor family and ligand binding leads to tyrosine phosphorylation of several cellular proteins via the Janus kinase (JAK)—signal transducers and activators of transcription 5 (STAT) pathway (42). In rabbits, prolactin increased the transport of potassium and decreased the transport of sodium across mammary epithelial cells (43). Prolactin has also been observed to increase the uptake of amino acids in the rat mammary gland (44). In rat intestinal epithelial membranes, there is a significant transfer of fluid and calcium stimulated by prolactin (45, 46, respectively). In the current study, Bromo treatment resulted in lower BAT mass in LD hamsters. Previous work has shown that in BAT, prolactin regulates UCP1 expression (47) and maintains thermogenic function (48). In white adipose tissue, prolactin regulates adipogenesis (49) and maintains fat deposition and leptin signaling (50). We also observed that 3 consecutive daily injections of prolactin were sufficient to increase kidney mass in hamsters. While the effects of prolactin on kidney mass have not been reported previously, prolactin infusions in rats significantly reduced urinary sodium, potassium, and water excretion (51). The observed changes in kidney mass may, therefore, reflect a long-term program to decrease water and electrolyte excretion and contribute to the increase in body mass.

Prolactin secretion from the pituitary is governed, in part, by tuberoinfundibular dopamine (TIDA) neurons expressed in the dorsomedial arcuate nucleus of the hypothalamus. These TIDA neurons signal via the D2 receptor (52) and function to inhibit the spontaneous electrical activity of lactotrophs and decrease prolactin release (53, 54). We used tyrosine hydroxylase, the rate-limiting enzyme for the synthesis of dopamine, as a proxy to examine long-term changes in prolactin regulation. *Th* expression was significantly elevated in short-day photoperiod hamsters, consistent with studies in seasonally breeding animals including sheep (55), golden hamster (56), and redheaded buntings (57). Somatostatin is

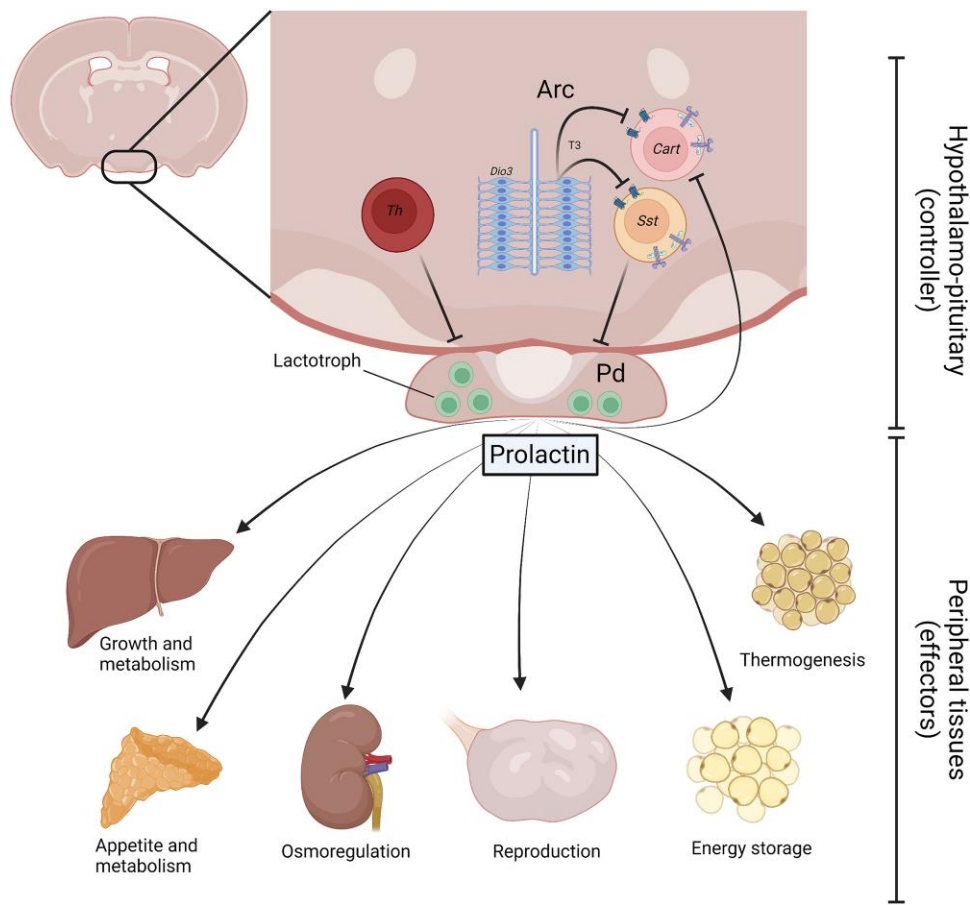


Figure 4. Model of programmed rheostatic regulation of seasonal body mass by prolactin. Annual set point in body mass is established by tanycytes along the third ventricle in the hypothalamus. Tanycyte expression of deiodinase type-3 (*Dio3*) governs the annual change in triiodothyronine (T3) production. T3 signals to adjacent neurons to convey time of year information to hypothalamic controllers of energy balance. Hypothalamic neurons expressing tyrosine hydroxylase (*Th*) and somatostatin are photoperiodically regulated and act as “controllers” of prolactin secretion from lactotrophs in the pars distalis. In the absence of inhibitory input, lactotrophs release prolactin into the circulatory system and act on multiple effector endocrine organs. Prolactin acts as a pleiotropic hormone to regulate energy storage, thermogenesis, reproduction, osmoregulation, growth, and metabolism. Prolactin is also necessary for short-feedback loops to inhibit cocaine- and amphetamine-regulated transcript (*Cart*) expression in the arcuate nucleus. Effector tissues (eg, adipose, liver) have well-characterized feedback mechanisms to regulate neuroendocrine control of energy balance. The figure was created using BioRender.

another neuropeptide that exerts inhibitory effects on prolactin secretion in mammals (27). Consistent with previous reports in hamsters (19), short photoperiod significantly increases *Sst* expression in the arcuate nucleus of the hypothalamus. The increase in both *Th* and *Sst* suggests that these 2 neuropeptides may regulate the release of prolactin from the pituitary gland.

Tanycytes are proposed to provide the long-term seasonal programmed change in body mass (12). In adult hamsters, *Dio3* expression is significantly upregulated in the ependymal layer of the third ventricle after prolonged exposure to short photoperiod (11, 58, 59). Here we confirm that *Dio3* expression is rapidly, and transiently upregulated in the short-day photoperiod condition (ie, SD3) (59). Thus, photoperiod-induced changes in triiodothyronine act to adjust the set point for the maintenance of seasonal body mass (12). Taken together, we propose that the seasonal regulation of body mass set point is established by a circannual timer residing in tanycytes and neuropeptides (ie, *Cart*, *Sst*) act as the controllers to regulate long-term changes in body mass.

Prolactin receptor is also expressed in the mediobasal hypothalamus, preoptic area, and choroid plexus in Siberian

hamsters and the sibling species *Phodopus campbelli* (60). Dense levels of *Prlr* expression are identified primarily in the arcuate nucleus and ventromedial nucleus in mice (61). Both *Sst* (19) and *Cart* (62) are expressed in the hamster arcuate nucleus and are significantly increased in short photoperiod conditions. Previous work using in situ hybridization found that the dorsomedial posterior arcuate nucleus has multiple transcripts that exhibit localized, photoperiodic changes in expression levels, including VGF nerve growth factor inducible, histamine H3 receptor, cellular retinoic acid binding protein-2, cellular retinol binding protein 1, retinoic acid receptor alpha, and retinoid X receptor gamma (see (63) for a review). This paper used a PCR-based approach to quantitatively assess transcript levels in a hypothalamic region that includes the arcuate nucleus and surrounding regions (eg, third ventricle). Consequently, the current study lacks the anatomical precision to identify any regional change of *Sst* and *Prlr* expression in the dorsomedial posterior arcuate nucleus. Recent single-cell sequencing in murine hypothalamus indicates co-localization of the prolactin receptor with both *Sst* and *Cart* expressing cells (64). Bromo-treated hamsters were found to have significantly increased *Cart* expression, but

there was no effect on *Sst* expression. Moreover, prolactin administration had no impact on either *Sst* or *Cart* expression. These findings indicate that prolactin is necessary, but not sufficient for the long photoperiod-induced inhibition of *Cart* expression.

There are a few limitations to the current work that are important to highlight. First, the studies only examined transcriptional regulation of mRNA expression and not translational or circulating levels of target hormones. Further work is required to assess the link between prolactin signaling and protein levels of anorexigenic and/or orexigenic neuropeptides. Second, it remains possible the effects of bromocriptine on body mass are mediated by other non-specific dopamine pathways. Bromocriptine has potent actions as a D2 receptor agonist and D1 receptor antagonist and is used to reduce growth hormone levels in patients with acromegaly (65). It remains possible that the reduction in body mass observed in Study 2 occurred in response to a reduction in circulating growth hormone levels in hamsters (24-26). Finally, radioimmunoassay has identified that plasma prolactin concentrations range from 100 to 600 ng/mL in Siberian hamsters (66). Unfortunately, the radioimmunoassay reagents for the assay could not be obtained and several enzyme-linked immunoassays were found to be nonspecific. Establishing changes in prolactin hormone during programmed rheostatic changes body mass will be important to examine the links between hormone signaling and changes in effector tissues.

Most research has focused on the role of prolactin in the hypothalamus to regulate parental behavior ((67); see (68) and (69) for reviews). The data provided here indicate that prolactin hormone is an output signal of the hypothalamus to control long-term programmed rheostatic regulation of body mass (Fig. 4). We show a strong positive relationship between the expression of prolactin mRNA and the increase in body mass during the onset of the annual interval timer. Then using daily bromocriptine injections, we show robust body mass loss that can be attributed to reduced circulating prolactin concentrations. Reduced body mass may be a result of increased hypothalamic *Cart* expression. Then we show that short-term administration of prolactin can increase body mass. Prolactin injections significantly increased kidney mass suggesting a potential link between lactotroph function and seasonal changes in osmoregulation. We propose that the photoperiod-induced changes in *Sst* and *Cart* act as the rheostatic controller of seasonal body mass and regulate the release of prolactin from the pituitary gland. Future studies are needed to (i) uncover the mechanistic link between *Sst* and *Cart* signaling to regulate prolactin mRNA expression; and (ii) determine tissue-specific effects of prolactin on peripheral tissues.

Acknowledgments

The research was funded by the Leverhulme Trust Research Leader award RL-2019-006 to T.J.S. The hamster icon used in Figs. 1-3 was obtained from BioRender. Figure 4 was created using BioRender Software.

Funding

The work was supported by Leverhulme Trust (RL-2019-06) to T.J.S.

Disclosures

The authors have nothing to declare.

Data Availability

All datasets generated during and/or analyzed during the current study are publicly available (38) or presented in Supplementary Table S2.

References

1. Cannon WB. *The Wisdom of the Body*. Norton and Company, Lnc.; 1963.
2. Riggs DS. *Control Theory and Physiological Feedback Mechanisms*. Williams and Wilkins; 1970.
3. Ebling FJP, Barrett P. The regulation of seasonal changes in food intake and body weight. *J Neuroendocrinol*. 2008;20(6):827-833.
4. Mrosovsk N. *Rheostasis: the Physiology of Change*. Oxford University Press; 1990.
5. Mercer JG, Speakman JR. Hypothalamic neuropeptide mechanisms for regulating energy balance: from rodent models to human obesity. *Neurosci Biobehav Rev*. 2001;25(2):101-116.
6. Yeo GS, Heisler LK. Unraveling the brain regulation of appetite: lessons from genetics. *Nat Neurosci*. 2012;15(10):1343-1349.
7. Van de Wall E, Leshan R, Xu AW, et al. Collective and individual functions of leptin receptor modulated neurons controlling metabolism and ingestion. *Endocrinol*. 2008;149(4):1773-1785.
8. Helfer G, Stevenson TJ. Pleiotropic effects of proopiomelanocortin and VGF nerve growth factor inducible neuropeptides for the long-term regulation of energy balance. *Mol Cell Endocrinol*. 2020;514:110876.
9. Mercer JG, Tups A. Neuropeptides and anticipatory changes in behaviour and physiology: seasonal body weight regulation in Siberian hamster. *Eur J Pharmacol*. 2003;480(1-3):43-50.
10. Lewis JE, Ebling FJP. Hamsters as model species for neuroendocrine studies. In: *Model Animals in Neuroendocrinology: from Worm to Mouse to man*: John Wiley & sons Ltd; 2022:161-179.
11. Bank JHH, Wilson D, Rijntjes E, Barrett P, Herwig A. Alternation between short- and long- photoperiod reveals hypothalamic gene regulation linked to seasonal body weight changes in Djungarian hamsters (*Phodopus sungorus*). *J Neuroendocrinol*. 2017;29(7). Doi: 10.1111/jne.12487
12. Barrett P, Ebling FJP, Schuhler S, et al. Hypothalamic thyroid hormone catabolism acts as a gatekeeper for the seasonal control of body weight and reproduction. *Endocrinol*. 2007;148(8):3608-3617.
13. Bartness TJ, Elliott JA, Goldman BD. Control of torpor and body weight patterns by a seasonal timer in Siberian hamsters. *Am J Physiol*. 1989;257(1 Pt 2):R142-R149.
14. Bao R, Onishi RG, Tolla E, et al. Genome sequencing and transcriptome analyses of the Siberian hamster hypothalamus identify mechanisms for seasonal energy balance. *Proc Natl Acad Sci*. 2019;116(26):13116-13121.
15. Bartness TJ, Hamilton JM, Wade GN, Goldman BD. Regional differences in fat pad responses to short days in Siberian hamsters. *Am J Physiol*. 1989;257(6 Pt 2):R1533-, R1540.
16. Lincoln G. A brief history of circannual time. *J Neuroendocrinol*. 2019;31(3):e12694.
17. Mercer JG, Lawrence CB, Beck B, Burlet A, Atkinson T, Barrett P. Hypothalamic NPY and prepro-NPY mRNA in Djungarian hamsters: effect of food deprivation and photoperiod. *Am J Physiol*. 1995;269(5 Pt 2):R1099-R1106.
18. Reddy AB, Cronin AS, Ford H, Ebling FJ. Seasonal regulation of food intake and body weight in the male Siberian hamster: studies of hypothalamic orexin (hypocretin), neuropeptide y (NPY) and pro-opiomelanocortin (POMC). *Eur J Neurosci*. 1999;11(9):3255-3264.

19. Rousseau K, Atcha Z, Cagampang FRA, *et al.* Photoperiodic regulation of leptin resistance in the seasonally breeding Siberian hamster (*Phodopus sungorus*). *Endocrinology*. 2002;143(8):3083-3095.
20. Herwig A, de Vries EM, Bolborea M, *et al.* Hypothalamic ventricular ependymal thyroid hormone deiodinases are an important element of circannual timing in the Siberian hamster (*Phodopus sungorus*). *PLoS One*. 2013;8(4):e62003.
21. Mercer JG, Ellis C, Moar KM, Logie TJ, Morgan PJ, Adam CL. Early regulation of hypothalamic arcuate nucleus CART gene expression by short photoperiod in the Siberian hamster. *Regul Pept*. 2003;111(1-3):129-136.
22. Barrett P, Ross AW, Balik A, *et al.* Photoperiodic regulation of histamine H3 receptor and VGF messenger ribonucleic acid in the arcuate nucleus of the Siberian hamster. *Endocrinology*. 2005;146(4):1930-1939.
23. Lisci C, Lewis JE, Daniel ZCTR, *et al.* Photoperiodic changes in adiposity increase sensitivity of female Siberian hamsters to systemic VGF derived peptide TLQP-21. *PLoS One*. 2019;14(8):e0221517.
24. Dumbell R, Petri I, Scherbarth F, *et al.* Somatostatin agonist pasireotide inhibits exercise-stimulated growth in the male Siberian hamster (*phodopus sungorus*). *J Neuroendocrinol*. 2017;29(1). Doi: [10.1111/jne.12448](https://doi.org/10.1111/jne.12448)
25. Dumbell RA, Scherbarth F, Diedrich V, Schmid HA, Steinlechner S, Barrett P. Somatostatin agonist pasireotide promotes a physiological state resembling short-day acclimation in the photoperiodic male siberian hamster (*phodopus sungorus*). *J Neuroendocrinol*. 2015;27(7):588-599.
26. Scherbarth F, Diedrich V, Dumbell R, Schmid HA, Steinlechner S, Barrett P. Somatostatin receptor activation is involved in the control of daily torpor in a seasonal mammal. *Am J Physiol Regul Integr Comp Physiol*. 2015;309(6):R668-R674.
27. Enjalbert A, Bertrand P, Le Dafniet M, *et al.* Somatostatin and regulation of prolactin secretion. *Psychoneuroendocrinology*. 1986;11(2):155-165.
28. Grattan DR, Kokay IC. Prolactin: a pleiotropic neuroendocrine hormone. *J Neuroendocrinol*. 2008;20(6):752-763.
29. Stewart C, Marshall CJ. Seasonality of prolactin in birds and mammals. *J Exp Zool A Ecol Integr Physiol*. 2022;337(9-10):919-938.
30. Ladyman SR, Augustine RA, Grattan DR. Hormone interactions regulating energy balance during pregnancy. *J Neuroendocrinol*. 2010;22(7):805-817.
31. Duncan MJ, Goldman BD. Hormonal regulation of the annual pelage color cycle in the Djungarian hamster, *phodopus sungorus*. II. Role of prolactin. *J Exp Zool*. 1984;230(1):97-103.
32. Bartness TJ, Wade GA, Goldman BD. Are the short-photoperiod induced decreases in serum prolactin responsible for the seasonal changes in energy balance in Syrian and Siberian hamsters? *J Exp. Zool*. 1987;244(3):437-454.
33. Lincoln GA, Clarke IJ, Hut RA, Hazlerigg DG. Characterizing a mammalian circannual pacemaker. *Science*. 2006;314(5807):1941-1944.
34. Stewart C, Hamilton G, Marshall CJ, Stevenson TJ. Transcriptome analyses of nine endocrine tissues identifies organism-wide transcript distribution and structure in the Siberian hamster. *Sci Rep*. 2022;12(1):13552.
35. Paul MJ, Probst CK, Brown LM, de Vries GJ. Dissociation of puberty and adolescent social development in a seasonally breeding species. *Curr Biol*. 2018;28(7):1116-1123.
36. Duncan MJ, Goldman BD. Physiological doses of prolactin stimulate pelage pigmentation in Djungarian hamster. *Am J Physiol*. 1985;248(6 Pt 2):R664-R667.
37. Coyle CS, Caso F, Tolla E, *et al.* Ovarian hormones induce de novo DNA methyltransferase expression in the Siberian hamster suprachiasmatic nucleus. *J Neuroendocrinol*. 2020;32(2):e12819.
38. Stevenson T. Data repository. *figshare*. *Journal Contribution*. 2023. Doi: [10.6084/m9.figshare.24534340](https://doi.org/10.6084/m9.figshare.24534340)
39. Stewart C, Liddle TA, Stevenson TJ. Abundance, efficiency, and stability of reference transcript expression in a seasonal rodent: the Siberian hamster. *PLoS One*. 2022;17(10):e0275263.
40. Zhao S, Fernald RD. Comprehensive algorithm for quantitative real-time polymerase chain reaction. *J. Comput Biol*. 2005;12(8):1047-1064.
41. Niklowitz P, Hoffmann K. Pineal and pituitary involvement in the photoperiodic regulation of body weight, coat color and testicular size of the Djungarian hamster, *Phodopus sungorus*. *Biol Reprod*. 1988;39(2):489-498.
42. Bole-Feysot C, Goffin V, Edery M, Binart N, Kelly PA. Prolactin (PRL) and its receptor: actions, signal transduction pathways and phenotypes observed in PRL receptor knockout mice. *Endo Rev*. 1998;19(3):225-268.
43. Falconer IR, Rowe JM. Possible mechanism for action of prolactin on mammary cell sodium transport. *Nature*. 1975;256(5515):327-328.
44. Vina J, Puertes IR, Saez GT, Vina JR. Role of prolactin in amino acid uptake by the lactating mammary gland of the rat. *FEBS Lett*. 1981;126(2):250-252.
45. Pahuja DN, DeLuca HF. Stimulation of intestinal calcium transport and bone calcium mobilization by prolactin in vitamin D-deficient rats. *Science*. 1981;214(4524):1038-1039.
46. Ramsey DH, Bern HA. Stimulation by ovine prolactin of fluid transfer in everted sacs of rat small intestines. *J Endocrinol*. 1972;53(3):453-459.
47. Lopez-Vicchi F, Ladyman SR, Ornstein AM, *et al.* Chronic high prolactin levels impact on gene expression at discrete hypothalamic nuclei involved in food intake. *FASEB J*. 2020;34(3):3902-3914.
48. Viengchareun S, Servel N, Fève B, Freemark M, Lombès M, Binart N. Prolactin receptor signaling is essential for perinatal brown adipocyte function: a role for insulin-like growth factor-2. *PLoS One*. 2008;3(2):e1535.
49. Nanbu-Wakao R, Fujitani Y, Masuho Y, Muramatsu M, Wakao H. Prolactin enhances CCAAT enhancer-binding protein- β (C/EBP β) and peroxisome proliferator-activated receptor γ (PPAR γ) messenger RNA expression and stimulates adipogenic conversion of NIH-3T3 cells. *Mol Endocrinol*. 2000;14(2):307-316.
50. Freemark M, Fleenor D, Driscoll P, Binart N, Kelly PA. Body weight and fat deposition in prolactin receptor-deficient mice. *Endocrinology*. 2001;142(2):532-537.
51. Stier CT Jr, Cowden EA, Friesen HG, Allison ME. Prolactin and the rat kidney: a clearance and micropuncture study. *Endocrinology*. 1984;115(1):362-367.
52. Kelly MA, Rubinstein M, Asa SL, *et al.* Pituitary lactotroph hyperplasia and chronic hyperprolactinemia in dopamine D2 receptor deficient mice. *Neuron*. 1997;19(1):103-113.
53. Gregerson KA. Functional expression of the dopamine-activated K⁺ current in lactotrophs during the estrous cycle in female rats: correlation with prolactin secretory responses. *Endocrine*. 2003;20(1-2):67-74.
54. De Greef WJ, Neill JD. Dopamine levels in hypophysial stalk plasma of the rat during surges of prolactin secretion induced by cervical stimulation. *Endocrinology*. 1979;105(5):1093-1099.
55. Vigué C, Thibault J, Thiéry JC, Tillet Y, Malpoux B. Photoperiodic modulation of monoamines and amino-acids involved in the control of prolactin and LH secretion in the ewe: evidence for a regulation of tyrosine hydroxylase activity. *J Neuroendocrinol*. 1996;8(6):465-474.
56. Steger RW, Juszczak M, Fadden C, Bartke A. Photoperiod effects on neurohypophyseal and tuberoinfundibular dopamine metabolism in the male hamster. *Endocrinology*. 1995;136(7):3000-3006.
57. Sharma A, Tripathi V, Kumar V. Hypothalamic molecular correlates of photoperiod-induced spring migration in intact and castrated male redheaded buntings. *Mol Cell Endocrinol*. 2023;561:111829.
58. Stevenson TJ, Prendergast BJ. Reversible DNA methylation regulates seasonal photoperiodic time measurement. *Proc Natl Acad Sci USA*. 2013;110(41):16651-16656.

59. Prendergast BJ, Pyter LM, Kampf-Lassin A, Patel PN, Stevenson TJ. Rapid induction of hypothalamic iodothyronine deiodinase expression by photoperiod and melatonin in juvenile Siberian hamster (*Phodopus sungorus*). *Endocrinology*. 2013;154(2):831-841.
60. Ma E, Lau J, Grattan DR, Lovejoy DA, Wynne-Edwards KE. Male and female prolactin receptor mRNA expression in the brain of a biparental and a uniparental hamster, *phodopus*, before and after the birth of a litter. *J Neuroendocrinol*. 2005;17(2):81-90.
61. Kokay IC, Wyatt A, Phillipps HR, et al. Analysis of prolactin receptor expression in the murine brain using a novel prolactin receptor reporter mouse. *J Neuroendocrinol*. 2018;30(9):e12634.
62. Khorooshi R, Helwig M, Werckenthin A, Steinberg N, Klingenspor M. Seasonal regulation of cocaine- and amphetamine-regulated transcript in the arcuate nucleus of Djungarian hamster (*Phodopus sungorus*). *Gen Comp. Endocrinol*. 2008;157(2):142-147.
63. Morgan PJ, Ross AW, Mercer JG, Barrett P. What can we learn from seasonal animals about the regulation of energy balance? *Prog Brain Res*. 2006;153:325-337.
64. Steuernagel L, Lam BYH, Klemm P, et al. HypoMap—a unified single-cell gene expression atlas of the murine hypothalamus. *Nat Metabol*. 2022;4(10):1402-1419.
65. Bell PM, Atkinson AB, Hadden DR, et al. Bromocriptine reduces growth hormone in acromegaly. *Arch Intern Med*. 1986;146(6):1145-1149.
66. Reburn CJ, Wynne-Edwards KE. Novel patterns of progesterone and prolactin in plasma during the estrous cycle in the Djungarian hamster as determined by repeated sampling of individual females. *Biol Reprod*. 1996;54(4):819-825.
67. Stagkourakis S, Smiley KO, Williams P, et al. A neuro-hormonal circuit for paternal behavior controlled by a hypothalamic network oscillation. *Cell*. 2020;182(4):960-975.e15.
68. Bridges RS, Grattan DR. 30 years after: CNS and prolactin: sources, mechanisms and physiological significance. *J Neuroendocrinol*. 2019;31(3):e12669.
69. Grattan DR. 60 years of neuroendocrinology: the hypothalamo-prolactin axis. *J Endocrinol*. 2015;226(2):T101-T122.